Original Article

Ultrasonographic and Computed Tomographic Anatomy of the Temporomandibular Joint in Goat (*Capra hircus*)

HebatAllah H. Mahmoud *, **Mohamed K. M. Abdel Maksoud and Azza A. H. Ibrahim**

Abstract

The temporomandibular joint (TMJ) has a complicated anatomical configuration that makes TMJ disease diagnosis challenging. The availability of ultrasonography and computed tomography (CT) in veterinary clinics has made the examination of this joint more feasible. The current study aimed to clarify the normal anatomical appearance of the TMJ in goats using ultrasonography and CT. The current study was conducted on 10 healthy adult goats of both sexes, aged 1-3.5 years and weighing 15-25 kg. The TMJs of six goats were examined using an ultrasonographic device with a 7.5 MHz linear probe. The cadaveric heads of the other four goats were examined using a multidetector helical computed tomography scanner. Ultrasonography provided high-quality images of the TMJ structures, including articular surfaces, joint cavity, joint capsule, and articular disc. CT allowed a brief visualization of the bony and soft tissues of the TMJ, providing superior discrimination of the bony elements and ligaments of this joint, which could not be clearly defined on ultrasonography. Additionally, the structures in the TMJ area, masticatory muscles, blood vessels, and parotid salivary gland could be depicted and defined on both ultrasonography and CT images. The annotated data provided a comprehensive anatomical description of the normal TMJ in goat using ultrasonography and CT to be a standard reference for further clinical diagnosis of this joint.

Keywords: Computed tomography (CT), Goat, Temporomandibular joint (TMJ), Ultrasonography

Department of Anatomy and Embryology, Faculty of Veterinary Medicine, Beni-Suef University, Beni-Suef 62511, Egypt

d.hebatallah@yahoo.com

1. Introduction

Goats are of great socio-economic importance, especially in developing countries. Recently, goats have become an essential aspect of animal production in Egypt, as they are considered a source of meat, milk, and hide (**Hamed et al., 2009**). Moreover, sheep and goats have recently been used as models in TMJ research to compare biological disorders associated with human TMJ diseases (**Angelo et al, 2016; El-Hady, 2020**). This suitability of small ruminants for studying TMJ is due to the similar bone and cartilage repair pattern in humans and small ruminants (**Ishimaru and Goss, 1992**). In addition, small ruminants are characterized by wide availability, low cost, and easy control (**Bifano et al., 1994**).

The temporomandibular joint is a characteristic feature of the Mammalia class that distinguishes mammals from other vertebrates (**Smith, 2001**). It is is a synovial articulation that includes the articular facet on the ventral surface of the zygomatic arch of the temporal bone, the head of the mandibular condyle of the mandible, the articular disc, dorsal and ventral synovial pouches, the joint capsule, and lateral and caudal ligaments (**Konig and Liebich 2009**). The movement of the temporomandibular joint is controlled by a group of strong muscles: the masseter, temporal, and pterygoid (**Porto et al., 2010**). These muscles help the TMJ achieve important mouth functions: chewing, deglutition, speech, yawning, and snoring (**Ingawale and Goswami, 2009**). Blood vessels, nerves, the middle ear, and the parotid salivary gland are other structures related to the TMJ (**Rodriguez et al., 2006**). Thus, the TMJ and its related structures form a complex anatomical region that is difficult to investigate in clinical problems of this joint (**Ramzan, 2006; Sparks et al., 2014**). Consequently, imaging modalities must be developed for a precise examination and further prognosis of the affected TMJ.

Traditional radiography is frequently used to image the TMJ abnormalities in cows and sheep; otherwise, it results in poor images of this joint due to the superimposition of the surrounding bony structures, the complex configuration of the area around the TMJ, and the inability to obtain

multiple imaging views (**Weller et al., 1999b; Nuss et al., 2011**). Ultrasonography is a widely available and commonly used primary diagnostic tool in veterinary clinics. This imaging modality allows the acquisition of valuable images of the periarticular soft structures, joint cavity, joint capsule, and articular surfaces (**Kofler et al., 2014; Borges et al., 2016**). However, ultrasonography is inadequate for examining deep and complicated structures (**Dyson et al., 2003**).

Computed tomography (CT) and magnetic resonance imaging (MRI) techniques have been advanced to overcome the overlapping of the anatomical structures, providing more reliable evaluation and accurate prognosis (**Devine et al., 2005; Nagy and Simhofer, 2006**). Due to its high peculiar resolution and three-dimensional reconstruction, CT has recently been used to assess osseous tissues, allowing an accurate visualization of the bone elements (**Greco et al., 2023**). Ultrasonography and computed tomography (CT) are extensively used to evaluate the TMJ in equine (**Rodriguez et al., 2007; Rodriguez et al., 2008; Carmalt et al., 2016; Pimentel and Carmalt, 2021; Lee et al., 2022**), camel (**Arencibia et al., 2012**), and bovine (**Kofler et al., 2014; Borges et al., 2016**); however, little attention has been paid to assessing the TMJ using these advanced techniques, especially in goats. The current study aimed to clarify the normal ultrasonographic and CT appearance of the TMJ in goats.

2. Materials and Methods

2.1. Animals

The current study was conducted on ten healthy adult goats of both sexes (five males and five females), aged 1-3.5 years and weighing 15-25 kg. Six goats were examined ultrasonographically, while the other four goats were slaughtered for reasons unrelated to this study, and their cadaveric heads were examined using computed tomography. Before the study, the animals were physically examined to ascertain that they showed no clinical signs related to TMJ disease. The Institutional Animal Care and Use Committee of Beni-Suef University, Egypt (BSU-IACUC-025-020) approved all animal procedures in this study.

2.2. Ultrasonographic examination

The goats ($n = 6$) were restrained and sedated with 0.5 mg/kg xylazine. HCl 2% (Xyla-Ject, ADWIA Co., SAE, Egypt) was added. To ensure the best possible transducer contact, the hair over the TMJ on both sides was shaved, cleansed with tap water, and covered by an acoustic gel. An ultrasonographic device (Mindray DP-10Vet, Mindray Bio-Medical Electronics Ltd., Shenzhen, Germany) fitted with a 7.5 MHz linear probe was used to examine the TMJ. All investigations were performed by one sonographer.

The TMJ area was defined and located by the following gross landmarks for better TMJ imaging: the zygomatic arch, the lateral canthus of the eye, the base of the ear, and the mandibular condyle. An imaginary line was drawn between the ear base and the lateral canthus of the eye. The probe was perpendicularly positioned on the zygomatic arch at the midway of the imaginary line, where the ventral tip of the probe remained on the condylar process of the mandible, while its dorsal tip rotated 45º caudally toward the base of the ear (**Figure 1**). The normal echogenicity of the bony surfaces, joint space, joint capsule, and the articular disc of the TMJ, and its surrounding structures, masticatory muscles, blood vessels, and parotid salivary gland were recorded and briefly described.

2.3. Computed tomography examination

The cadaveric heads were examined using a multidetector helical CT scanner (Alexion Toshiba; Philips Siemens, Japan). The CT settings were 150 mA, 100 kV, and 1 ml slice thickness. The heads were scanned in a rostral to caudal direction from the orbit to the occipital bone level. The images were obtained in transverse and sagittal planes to be reconstructed into a bone window (window level 350 HUs and window width 3500 HUs) and a tissue window (window level 40 HUs and window width 400 HUs). The acquired images were serially numbered and grossly inspected, and the tissue density of the structures in the TMJ area was recorded.

3. Results
3.1. Ultrasonography

The TMJ components could be clearly identified sonographically using a linear-array probe. The articular surfaces of the temporal bone zygomatic process and the mandible condylar process ap-
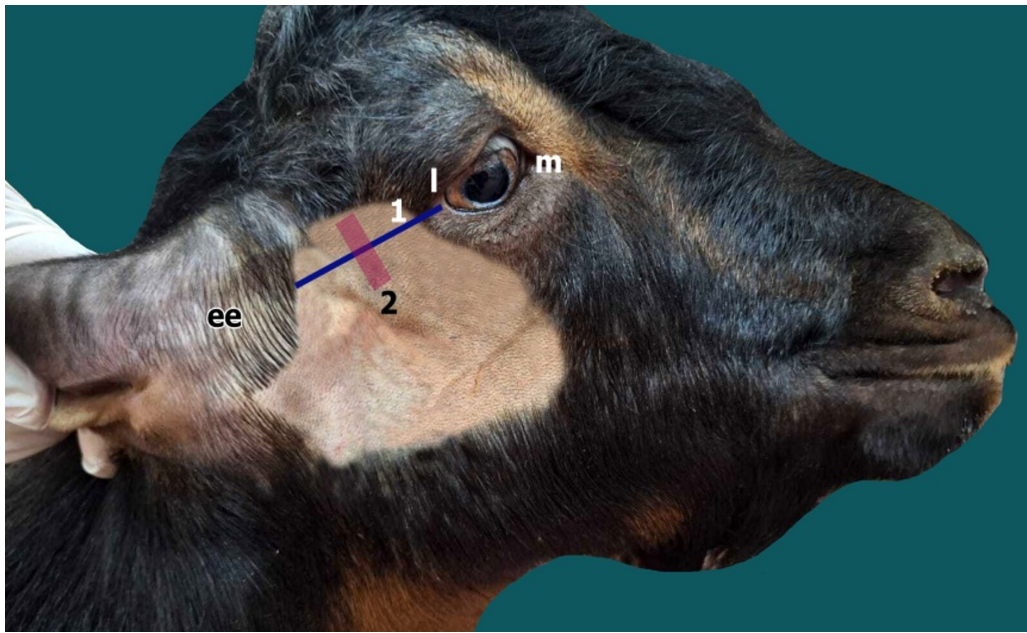
Figure 1: The right surface of the adult male goat's head shows the external ear (ee), lateral canthus of the eye (l), medial canthus of the eye (m), the line drawn from the ear's base to the lateral canthus of the eye (1), and the drawn rectangular (2), which indicates the position of the probe perpendicular to the drawn line and its dorsal tip rotated 45º toward the ear's base.
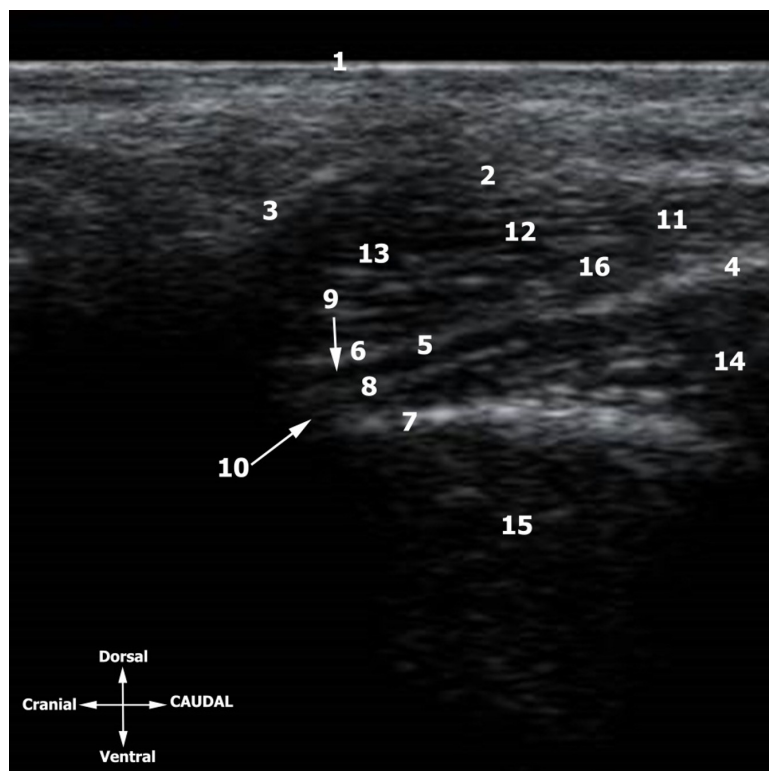

Figure 2: Ultrasonographic image of the temporomandibular joint (TMJ) in a healthy adult goat, obtained using B-mode ultrasonography with a 6 MHz convex probe. The images are as follows: 1- skin, 2- temporal muscle, 3- coronoid process of the mandible, 4- squamous part of temporal bone, 5- zygomatic process of temporal bone, 6- articular tubercle, 7- condylar process of the mandible, 8- articular disc, 9- joint cavity of the TMJ, 10- joint capsule, 11- zygomatico-auricular muscle, 12- superficial temporal artery, 13- superficial temporal vein, 14- parotid salivary gland, 15- masseter muscle, and 16- zygomatico-auricular muscle.
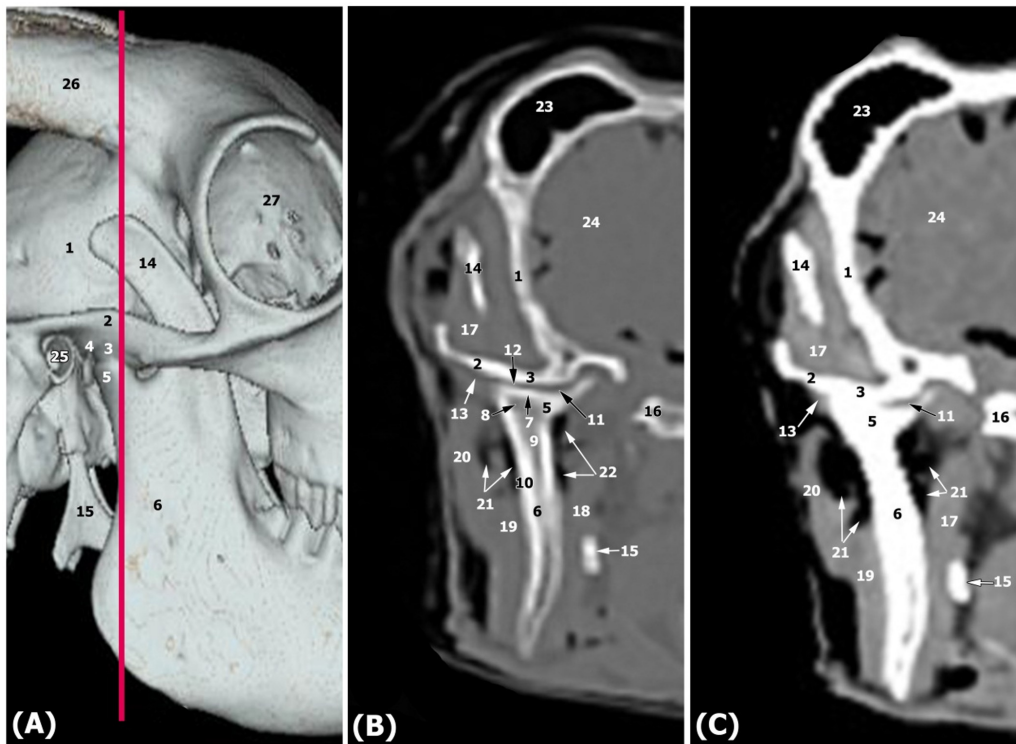
Figure 3: Three-dimensional reformatted computed tomographic image of the lateral aspect of the right temporomandibular joint (A) showing the transverse plane (red line) which refers to its corresponding transverse bone window (B), and tissue window (C) computed tomographic images of the right temporomandibular joint in goat. 1- parietal bone, 2- zygomatic process of temporal bone, 3- articular tubercle, 4- retroarticular process, 5- condylar process of the mandible, 6- ramus of the mandible, 7- articular cartilage, 8- subchondral bone, 9- spongy bone of mandible, 10- cortical bone of mandible, 11- articular disc, 12- dorsal synovial pouch of the TMJ, 13- lateralligament of the TMJ, 14- coronoid process of the mandible, 15- stylohyoid process, 16- basisphenoid bone, 17- temporal muscle, 18- lateral pterygoid muscle, 19- masseter muscle, 20- parotid salivary gland, 21- transverse facial vessels, 22- buccal vein, 23- corneal diverticulum of the frontal sinus, 24- brain, 25- external acoustic meatus, 26- corneal process of frontal bone, 27- orbital cavity.

peared as hyperechoic linear structures. The articular tubercle of the temporal bone could be depicted with a slight concave contour, especially toward the joint space. In adaptation, the articular disc could be visualized as a thin echogenic line between the articular surfaces of the temporal bone zygomatic process and the mandible condylar process.

The articular capsule was delineated as a small echogenic structure close to the lateral border of the condylar process of the mandible. Induction of slight chewing movement during sonographic examination enabled better visualization of the TMJ joint cavity. Dorsal to the articular disc, the joint space of the dorsal synovial pouch appeared as a hypoechoic space, while the ventral synovial pouch could not be recognized sonographically. It is important to clarify that the lateral and caudal ligaments of the TMJ could not be depicted using ultrasonography (**Figure 2**).

Differentiating and categorizing all the blood vessels around the TMJ using ultrasonography

was difficult. However, the large blood vessels, such as the superficial temporal vessels, could be identified as tubular hypoechoic structures surrounded by faint echogenic lines dorsolateral to the TMJ. Moreover, the large muscles, including the temporal, masseter, and zygomaticoauricular muscles, appeared as heterogeneous hypoechoic structures with demarcated heterogeneous hyperechoic branches, indicating the septa between these muscles. Further caudal to the TMJ at the base of the ear, the parotid salivary gland could be outlined as a heterogeneous hypoechoic structure with echogenic dots indicating the internal lobular architecture of this gland (**Figure 2**).

3.2. Computed tomography of the TMJ

Computed tomography with its windows, bone, and tissue, provided a comprehensive and detailed visualization of the TMJ bone and soft tissues. Bone window computed tomography (CT) images enabled better differentiation and delin-
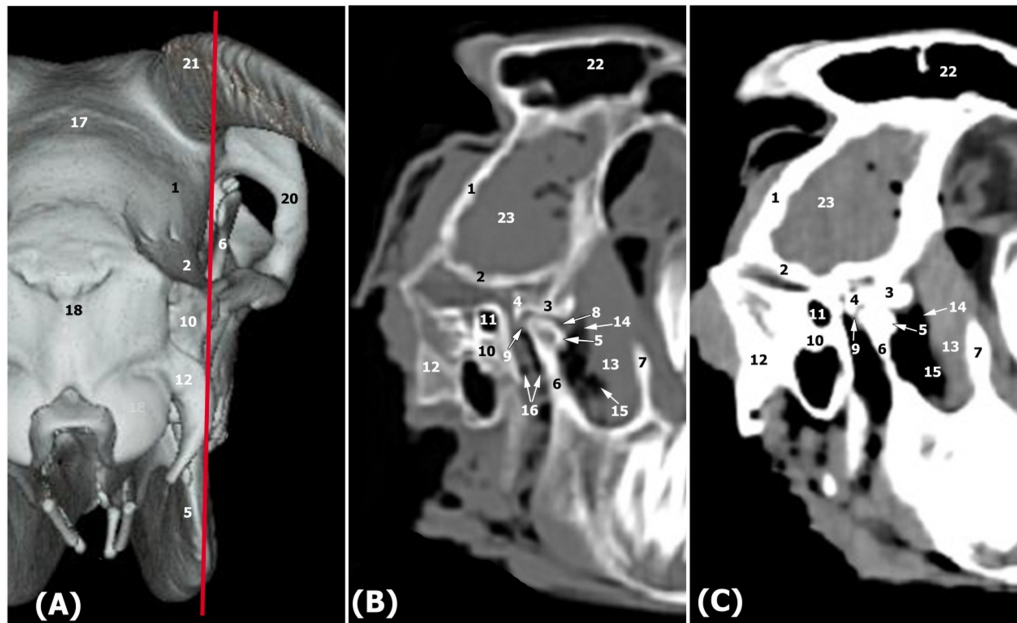
Figure 4: Three-dimensional reformatted computed tomographic image of the caudolateral aspect of the right temporomandibular joint (A) showing the transverse plane (red line) which refers to its corresponding transverse bone window (B), and tissue window (C) computed tomographic images of the right temporomandibular joint in goat. 1- parietal bone, 2- squamous part of the temporal bone, 3- articular tubercle, 4- retroarticular process, 5- mandibular condyle, 6- ramus of mandible, 7- coronoid process of the mandible, 8- articular disc, 9- caudal ligament of the TMJ, 10- petrous bone (squamous part), 11- external acoustic meatus, 12- precondylar process, 13- lateral pterygoid muscle, 14- mandibular nerve, 15- buccal vein, 16- transverse facial vessels, 17- interparietal bone, 18- occipital bone, 19- occipital condyle, 20- zygomatic arch, 21- corneal process of the frontal bone, 22- corneal diverticulum of the frontal sinus, 23- brain

eation of the hard structures of the TMJ, including the articular surfaces, cartilage, and disc. The articular tubercle on the ventral surface of the temporal bone zygomatic process, the retroarticular process, and the head of the mandibular ramus condylar process exhibited a hyperdensity appearance on CT images. The articular surfaces were covered by a thin line of hyperdense articular cartilage. The subchondral bone was clearly visualized as a homogenous, intermediately dense area under the articular cartilages.

In addition, on bone window CT images, it was possible to differentiate between the cortical and spongy bones of the ramus of the mandible, where the cortical bone appeared as a hyperdense structure and the spongy bone appeared with heterogeneous intermediate density. Furthermore, the articular disc could be seen with an intermediate density between the articular surfaces at the TMJ periphery (**Figures 3 and 4**).

The lateral ligament of the TMJ was easily identified on the transverse CT image running parallel to the transverse section of the zygomatic process of the temporal bone (**Figure 3**). The caudal ligament could be depicted on the sagittal CT image extending from the condylar process of the mandibular ramus to the retroarticular pro-

cess (**Figure 4**). These ligaments exhibited an intermediate density on computed tomography images. Around the TMJ, several blood vessels, including the transverse facial vessels lateral to the ramus of the mandible and tributaries of the buccal vein between the lateral pterygoid muscle and the ramus of the mandible, could be depicted as rounded hypodense areas. In addition, the masticatory muscles could be clearly delineated: the temporal, masseter, and lateral pterygoid muscles, which appeared with heterogeneous intermediate density (**Figures 3, 4**). Furthermore, the parotid salivary gland could be outlined with heterogeneous intermediate density covering the lateral aspect of the masseter muscle on the transverse CT image (**Figure 4**).

4. Discussion

The TMJ is a fundamental part of the orofacial system, representing the central component of this system, and it shows great coordination in shape and function features (**Patil and Bindra, 2012**). Understanding the normal morphology and imaging characteristics of the TMJ is crucial for obtaining an accurate prognosis and diagnosis of several mouth disorders. However, the

complexity of the TMJ with its closely associated tissues makes TMJ assessment challenging. The current report provided a comprehensive and detailed imaging description of the TMJ using ultrasonography and CT, which could assist in the future evaluation of TMJ disorders in goats.

TMJ imaging techniques have undergone several developmental steps in the last 2 decades. Traditional radiography is the most common and primary tool for TMJ examination in horses (**Ramzan, 2006**), cows (**Sparks et al., 2014**), and sheep (**Arthur et al., 2015**). Ultrasound with a 7.5 MHz linear probe is becoming a routine imaging technique in veterinary clinics because it is a cheap, non-invasive diagnostic method that can be applied to standing animals with a rare need for sedation (**Kofler 2009; Kofler et al. 2014**). Moreover, CT, with its high-contrast imaging quality of both soft and bone tissues, is becoming a pragmatic choice for the evaluation of the TMJ (**Lee et al., 2022**).

The ultrasonographic examination of the TMJ in goats followed the protocol designed by **Rodriguez et al. (2007)** and **Borges et al. (2016)** for horses and bovines, respectively, where the linear probe was obliquely positioned on an imaginary line between the base of the ear and lateral canthus of the eye, and its dorsal tip rotated 45º toward the base of the ear. This technique enabled the imaging and identification of the TMJ bone contours, the temporal zygomatic arch, the retroarticular process, the mandible condylar process, and the closely related structures, such as blood vessels, muscles, and salivary glands.

Furthermore, the use of a linear probe enabled the depiction of the dorsal synovial pouch of the TMJ between the articular surface of the zygomatic process and the articular disc, which could be facilitated by the induction of a slight chewing movement during sonographic investigation. Although the ventral synovial pouch could not be seen on ultrasonographic images, this might be due to its smaller size than the dorsal one (**Rodriguez et al., 2006**). In contrast, these synovial pouches could not be visualized using a linear probe in previous ultrasonographic findings in horses (**Weller et al., 1999a; Rodriguez et al., 2007**) and bovines (**Kofler, 2000; Borges et al., 2015; Borges et al., 2016**). However, the use of a convex probe in bovine with a high frequency of 7.5 MHz facilitated imaging of the articular disc and the joint cavity (**Borges et al., 2016**).

The differences in the ability to visualize the joint cavity of the TMJ might be attributed to some factors, including frequencies of the applied probe (**Blond and Buczinski, 2009**), the experience level of the sonographer, individual animal variations, and the ability to induce slight chewing movement during examination (**Borges et al., 2016**). Moreover, on application of the linear probe ultrasonography, the joint capsule and synovial pouches can be clearly differentiated from the articular bone contours in bovine cases showing inflammatory effusion (**Borges et al., 2016**). These ultrasonographic findings potentiate the application of a 7.5 MHz linear probe for the assessment of several TMJ pathologies (**Kofler, 2009; Arthur et al., 2015**).

Ultrasonographic examination of the TMJ in goat revealed a close adjuncture of this joint to the superficial temporal vessels. These detailed images of relatively large blood vessels are considered vital and crucial information for veterinary surgeons during therapeutic intervention within the TMJ using arthroscopy (**May et al., 2001**) or condylectomy induction (**Sparks et al., 2014**).

In this study, a high-resolution multidetector helical CT scanner provided comprehensive discrimination and excellent visualization of the bone and soft tissues composing the TMJ in goats. The relevant anatomical structures of the TMJ were clearly identified using two CT views, i.e., transverse and sagittal views. The articular surfaces and articular disc were delineated on both transverse and sagittal CT images; the articular cavity and lateral ligament were best depicted on the transverse CT image, while the sagittal CT image best visualized the retroarticular process and the caudal ligament. These findings were in line with those of **Yu et al. (2004)** and **Casanova et al. (2006)** in humans, where the transverse and sagittal views are highly recommended to assess the TMJ structures. Furthermore, the volumetric three-dimensional reconstructed CT images in the current study enabled comprehensive visualization of the articular surfaces and bony landmarks of the TMJ, which helped in the identification of the osseous elements of the TMJ on bone window CT images.

Bone window CT provided good-quality images of the hard structures constituting the TMJ, including the articular cartilage, subchondral bone, cortical bone, and cancellous structures that could not be identified on ultrasono-

graphic images. In addition, the obtained three-dimensional reconstructed images enabled the depiction of the relevant anatomical structures in multiple views. These advantages of CT images enable clinicians to detect osseous alterations before their clinical appearance (**Young et al., 2007**), which could greatly assist in the diagnosis and prognosis of orthopedic diseases (**Raji et al., 2008**).

The articular disc is a vital component of the TMJ that aids in congruence between the articular surfaces of the TMJ, disperses masticatory force, reduces articular cartilage damage, and prevents the wear of this cartilage (**Tanaka et al., 2008**). This disc could be clearly delineated at the TMJ periphery on transverse and sagittal CT images. The limited visualization of the articular disc at the periphery of the joint might be due to its anatomical configuration, where the disc is thick peripherally and thin centrally, as observed in sheep (**El-Hady, 2020**) and horses (**Rodriguez et al., 2006**).

Moreover, the tissue window CT facilitated a clear visualization of the soft tissues of the TMJ in goats with variable tissue densities. Similar to the ultrasonographic findings, the dorsal synovial pouch could be depicted on the transverse CT image, whereas the small ventral pouch could not be seen. The lateral ligament of the TMJ was visualized on the transverse CT image, while the caudal ligament was visualized on the sagittal CT image. These ligaments could not be identified on the ultrasonographic images in the current study. In contrast, in previous CT images, the dorsal synovial pouch was faintly seen, and the ligaments could not be delineated, as recorded in horses (**Rodriguez et al., 2006**) and sheep (**El-Hady, 2020**). Moreover, as reported by **Rodriguez et al. (2008)** and **Arencibia et al. (2012)**, the close adjoining soft tissues were precisely visualized with variable densities on CT images, including the masticatory muscles, blood vessels, and nerves.

5. Conclusion

Although ultrasonography is the most realistic and feasible imaging technique for veterinary clinicians, computed tomography (CT) remains the most accurate diagnostic imaging modality for the examination of the TMJ. The ultrasonographic and CT images obtained in the current investigation provided a standard reference guide for future clinical studies of the TMJ in goats.

6. References

Angelo DF, Morouço P, Alves N, Viana T, Santos F, González R, Monje F, Macias D, Carrapiço B, Sousa R, Cavaco-Gonçalves S, Salvado F, Peleteiro C, Pinho M (2016). Choosing sheep (Ovis aries) as animal model for temporomandibular joint research: Morphological, histological and biomechanical characterization of the joint disc. Morphol., 100(331): 223-233. Doi: http://dx.doi.org/10.1016/j.morpho.2016.06.002

Arencibia A, Blanco D, Gonzalez N, Rivero MA (2012). Computed tomography and magnetic resonance imaging features of the temporomandibular joint in two normal camels. Anat Res Int., 242065. Doi: http://dx.doi.org/10.1155/2012/242065

Arthur C, Watt K, Nussey DH, Pemberton JM, Pilkington JG, Herman JS,Timmons ZL, Clements DN, Scott PR (2015). Osteoarthritis of the temporomandibular joint in free-living Soay sheep on St Kilda. Vet J., 203(1): 120-5. Doi: http://dx.doi.org/10.1016/j.tvjl.2014.10.014

Bifano C, Hubbard G, Ehler W (1994). A comparison of the form and function of the human, monkey, and goat temporomandibular joint. J Oral Maxillofac Surg., 52(3): 272-275. Doi: http://dx.doi.org/10.1016/0278-2391(94)90298-4

Blond L, Buczinski S (2009). Basis of ultrasound imaging and the main artifacts in bovine medicine. Vet. Clin. North Am. Food Anim. Pract., 25(3): 553-565. Doi: http://dx.doi.org/10.1016/j.cvfa.2009.07.002

Borges NC, Weissengruber G, Huber J, Kofler J (2015). Ultrasonographic examination of the elbow joint in calves and cows – normal appearance. Berl Munch Tierarztl Wochenschr., 128(9-10): 416–424. Doi: https://pubmed.ncbi.nlm.nih.gov/26591389/

Borges NC, Weissengruber GE, Huber J, Kofler J (2016). Ultrasonographic imaging of the temporomandibular joint in healthy cattle and pathological findings in one clinical case. N Z Vet J., 64(6): 330-336. Doi: http://dx.doi.org/10.1080/00480169.2016.1207575

Carmalt JL, Kneissl S, Rawlinson JE, Zwick T, Zekas L, Ohlerth S, Bienert-zeit A (2016). computed tomographic appearance of the temporomandibular joint in 1018 asymptomatic horses: a multi-institution study. Vet Radiol Ultrasound., 257(3): 237-245. Doi: http://dx.doi.org/10.1111/vru.12334

Casanova MS, Tuji FM, Ortega AI, Yoo HJ, Haiter-Neto F (2006). Computed tomography of the TMJ in diagnosis of ankylosis: two case reports. Med. oral Pathol. oral Cir. Bucal., 11(5): E-413-416. Doi: https://pubmed.ncbi.nlm.nih.gov/16878058/

Devine DV, Moll HD, Bahr RJ (2005). Fracture, luxation, and chronic septic arthritis of the temporomandibular joint in a juvenile horse. J vet Dent., 22(2): 96-99. Doi: http://dx.doi.org/10.1177/089875640502200204

Dyson S, Murray M, Schramme M, Branch M (2003). Magnetic resonance imaging of the equine foot: 15 horses. Equine Vet J., 35(1): 18–26. Doi: https://doi.org/10.2746/042516403775467531

El-Hady E (2020). The suitability of the egyptian baladi sheep (ovis aries) as a large animal model for temporomandibular joint studies. Int J Adv Res., 8(04): 259-269. Doi: http://dx.doi.org/10.21474/IJAR01/10775

Greco A, Meomartino L, Gnudi G, Brunetti A, Di Giancamillo M (2023). Imaging techniques in veterinary medicine. Part II: Computed tomography,magnetic resonance imaging, nuclear medicine. Eur J Radiol Open, 10: 1-21. Doi: https://doi.org/10.1016/j.ejro.2022.100467

Hamed A, Mabrouk MM, Shaat I, Bata S (2009). Esti-

mation of genetic parameters and some non-genetic factors for litter size at birth and weaning and milk yield traits in zaraibi goats. Egypt. J of Sheep Goat Sci., 4(2): 55-64. Doi: http://dx.doi.org/10.21608/EJSGS.2009.27667

Ingawale S, Goswami T (2009). Temporomandibular joint: disorders, treatments, and biomechanics. Ann Biomed Eng., 37(5): 976-996. Doi: http://dx.doi.org/10.1007/s10439-009-9659-4

Ishimaru J, Goss AN (1992). A model for osteoarthritis of the temporomandibular joint. J Oral Maxillofac Surg., 50(11): 1191-1195. Doi: http://dx.doi.org/10.1016/0278-2391(92)90153-q

Kofler J (2000). Ultrasonographic examination of the carpal region in cattle – normal appearance. Vet. J., 159(1), 85-96. Doi: http://dx.doi.org/10.1053/tvjl.1998.0339

Kofler J (2009). Ultrasonography as a diagnostic aid in bovine musculoskeletal disorders. Vet. Clin. North Am. Food Anim. Pract., 25: 687-731. Doi: http://dx.doi.org/10.1016/j.cvfa.2009.07.011

Kofler J, Geissbühler U, Steiner A (2014). Diagnostic imaging in bovine orthopedics. Vet. Clin. North Am. Food Anim. Pract., 30(1): 11-53. Doi: http://dx.doi.org/10.1016/j.cvfa.2013.11.003

Konig HE, Liebich HG (2009). Veterinary anatomy of domestic mammals. 3rd ed. Germany: Scattauerc GmbH, Stuttgart, pp. 595-603. Doi: https://www.wava-amav.org/downloads/koenig_liebich.pdf

Lee S, Lee EB, Park KW, Jeong H, Shin KY, Kweon YP, Seo JP (2022). Computed tomographic features of the temporomandibular joint in 10 Jeju horses. J Vet Sci., 23(3): e44. Doi: http://dx.doi.org/10.4142/jvs.21318

May KA, Moll HD, Howard RD, Pleasant RS, Gregg JM (2001). Arthroscopic anatomy of the equine temporomandibular joint. Vet. Surg. 30(6): 564-571. Doi: http://dx.doi.org/10.1053/jvet.2001.28438

Nagy AD, Simhofer H (2006). Mandibular condylectomy and meniscectomy for the treatment of septic temporomandibular joint arthritis in a horse. Vet Surg., 35(1): 663-668. Doi: http://dx.doi.org/10.1111/j.1532-950X.2006.00205.x

Nuss K, Schnetzler C, Hagen R, Schwarz A, Kircher P (2011). Clinical application of computed tomography in cattle. Tierarztl Prax Ausg G Grosstiere Nutztiere., 39(5): 317–324. Doi: https://pubmed.ncbi.nlm.nih.gov/22134604/

Patil AS, Bindra GK (2012). Morphology of the Temporomandibular Joint (TMJ) of Sheep (Ovis aries). Open J Vet Med., 2(4): 242-244. Doi: http://dx.doi.org/10.4236/ojvm.2012.24039

Pimentel KL, Carmalt JL (2021). The Frequency of Communication Between the Synovial Compartments of the Equine Temporomandibular Joint: A Contrast-Enhanced Computed Tomographic Assessment. Front Vet Sci., 8:753983. Doi: http://dx.doi.org/10.3389/fvets.2021.753983

Porto GG, Vasconcelos BC, Andrade ES, Silva-Junior VA (2010). Comparison between human and rat TMJ: anatomic and histopathologic features. Acta Cir Bras., 25(3): 290-293. Doi: https://doi.org/10.1590/S0102-86502010000300012

Ramzan PHL (2006). The temporomandibular joint: component of clinical complexity. Equine vet. J. 38(3): 102-104.

Doi: https://doi.org/10.2746/042516406776563323

Raji AR, Sardari K, Mohammadi HR (2008). Normal cross-sectional anatomy of the bovine digit: Comparison of computed tomog raphy and limb anatomy. Anat Histol Embryol., 37(3): 188-191. Doi: https://doi.org/10.1111/j.1439-0264.2007.00825.x

Rodriguez MJ, Agut A, Gil F, Latorre R (2006). Anatomy of the equine temporomandibular joint: study by gross dissection, vascular injection and section. Equine vet J., 38(2): 143-147. Doi: https://doi.org/10.2746/042516406776563378

Rodriguez MJ, Soler M, Latorre R, Gil F, Agut A (2007). Ultrasonographic anatomy of the temporomandibular joint in healthy Pure Bred Spanish horses. Vet. Radiol. Ultrasound, 48(2): 149-154. Doi: https://doi.org/10.1111/j.1740-8261.2007.00223.x

Rodriguez MJ, Latorre R, Lopez-Albors O, Soler M, Aguirre C, Vazquez JM, Querol M, Agut A (2008). Computed tomographic anatomy of the temporomandibular joint in the young horse. Equine vet J., 40(1): 1-6. Doi: https://doi.org/10.2746/042516408X322166

Smith KK (2001). The evolution of mammalian development. Bull Mus Comp Zool., 156: 119-135. https://www.researchgate.net/publication/312978221_The_evolution_of_mammalian_development

Sparks HD, Roquet I, Mackay A, Barber S (2014). Mandibular condylectomy in a cow with a chronic luxation of the temporomandibular joint. Can Vet J., 55(6): 577–581. Doi: https://pmc.ncbi.nlm.nih.gov/articles/PMC4022028/

Tanaka E, Detamore MS, Tanimoto K, Kawai N (2008). Lubrication of the temporomandibular joint. Ann Biomed Eng., 36(1):14-29. Doi: http://dx.doi.org/10.1007/s10439-007-9401-z

Weller R, Taylor S, Maierl J, Cauvin E, May S (1999a). Ultrasonographic anatomy of the equine temporomandibular joint. Equine vet. J. 31(6): 529-532. Doi: https://doi.org/10.1111/j.2042-3306.1999.tb03863.x

Weller R, Cauvin ER, Bowen IM, May SA (1999b). Comparison of radiography, scintigraphy and Ultrasonography in the diagnosis of a case of temporomandibular joint arthropathy in a horse. Vet. Rec. 144(14): 377-379. Doi: https://doi.org/10.1136/vr.144.14.377

Young BD, Samii VF, Mattoon JS, Weibrode SE, Bertone AL (2007). Subchondral bone bdensity and cartilage degeneration patterns in osteoarthritic metacarpal condyles of horses. Am J Vet Res., 68(8): 841–849. Doi: https://doi.org/10.2460/ajvr.68.8.841

Yu Q, Yang J, Wang P, Shi H, Luo J (2004). CT features of synovial chondromatosis in the temporomandibular joint. Oral Surg. oral Med. Oral Pathol. 97(4): 524-528. Doi: https://doi.org/10.1016/j.tripleo.2003.10.027